Industrial Combustion
Journal of the International Flame Research Foundation
Article Number 201603, December 2016
ISSN 2075-3071

CFD modelling of pulverized coal combustion in a blast furnace test rig

Ari Vuokila[1*], Olli Mattila[2], Riitta L. Keiski[1], Esa Muurinen[1]

[1]*University of Oulu, Pentti Kaiteran katu 1, 90014, Oulu, Finland*

[2]*SSAB Europe, Rautaruukintie 155, P.O.Box 93, 92101, Raahe, Finland*

[*] *Corresponding author. Email address:ari.vuokila@oulu.fi*

Abstract – Pulverized coal is the most common auxiliary fuel used in blast furnaces. Auxiliary fuels are used to replace expensive coke as a reducing agent for iron oxides. High amounts of pulverized coal injection lead to permeability changes in a blast furnace shaft together with an excess amount of unburnt coal. Permeability issues can be tackled with an adjusted charging program, but poor pulverized coal combustion will not enable cost efficient substitution of coke with coal. The only way to overcome this limit is to improve the conditions in pulverized coal combustion. The aim of this study was to create a combustion model for pulverized coal, which could be used to locate limiting factors in auxiliary fuel combustion in the actual blast furnace. Experimental results were used to validate the combustion model. The CFD model had a good agreement with experimental results with different types of coals. According to this study, this kind of combustion model can be used to study the blast furnace operation.

1. Introduction

The blast furnace is the most commonly used technology to produce pig iron. It is a shaft furnace, where in the case of the Raahe blast furnace, iron ore pellets and briquettes are charged from the top with the primary fuel coke. Auxiliary fuels (pulverized coal (PC), natural gas, heavy oil, tar, etc.) are injected into a blast furnace to reduce consumption of expensive coke, to decrease carbon dioxide emissions (through a higher H/C ratio), to stabilize the process and to increase productivity. Auxiliary fuels can replace coke in two ways, i.e. as a reducing agent for iron oxides, and by providing energy for the blast furnace operation [1].

Pulverized coal injection (PCI) is used in the company SSAB's Raahe mill blast furnaces, because of the high price of extra heavy oil. Combustion and gasification of the PC have to be optimized, because unburnt coal lowers the permeability of gases in the blast furnace. With low combustion efficiency, fine coal char accumulates on the surface of the hearth coke called the Deadman (Fig. 1) and makes it difficult to maintain stable blast furnace operation [2].

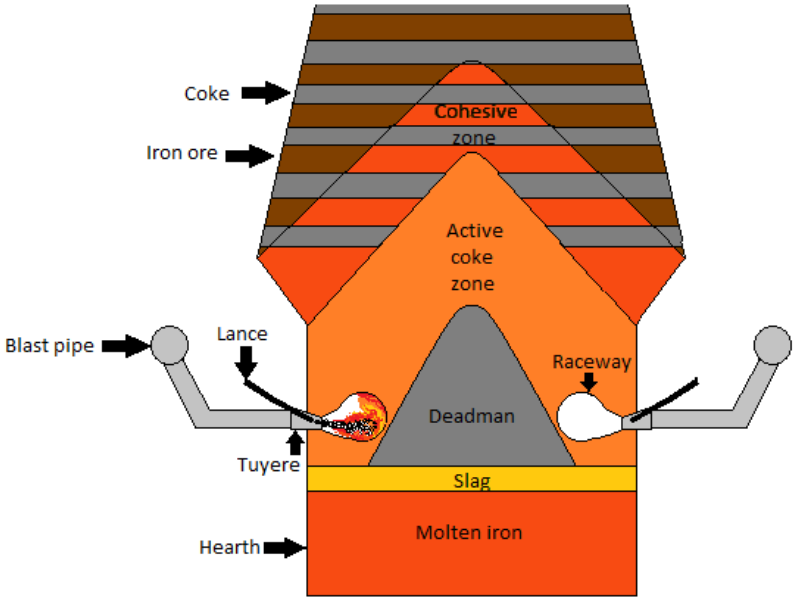

Figure 1. Schematic picture of the bottom part of blast furnace.

In a blast furnace, nozzles, called tuyeres, are used to blow hot air blast into the lower part of furnace to provide oxygen needed for combustion and gasification of coke and hydrocarbons. Air blast forms cavity, called raceway, in the coke bed in front of the tuyere. The auxiliary fuel such as PC is injected into the air blast through lance in a tuyere.

In the tuyere-raceway area of a blast furnace, experimental measurements are extremely difficult to take due to the harsh environment (high temperature, increased pressure and solid and molten materials), which creates the need for alternative research methods [3]. Computational fluid dynamics (CFD) modelling is chosen to study combustion and gasification of PC. Typically, these combustion models use only diffusion limited combustion models like the Eddy Dissipation Model (EDM) [4,5] or the Eddy breakup model (EBU) [6,7]. These kinds of models do not apply very well in blast furnaces because the temperatures are around 2800 K and oxygen levels are from 0.5 to 0.8 [2] of the stoichiometric ratio, which means that gasification reactions are important. Mixed-is-burnt models are not temperature dependent, which might lead to overestimation of PC burnout in the centre parts of the air blast, where temperatures are low due to devolatilization and poor mixing between the fuel and the air blast [1].

To overcome the shortcomings of the old models, the aim of this study was to create a combustion model for PC that is accurate enough to capture limiting factors of the injection process and can be used to improve injection methods in the tuyere area. Combustion of coal can be divided into five stages: heating, drying, devolatilization, volatile combustion and residual char combustion. An extensive model is needed for volatile combustion due to the high temperature and rich air-fuel mixture. The residual char combustion is described with reactions between char, oxygen, carbon dioxide and steam. The CFD model is created based on an experimental rig at BHP Billiton-BlueScope Steel [11] and the CFD model is validated with experimental results found from the literature [7].

2. Model description

The blast furnace in SSAB steel factory in Raahe, Finland, which has 21 tuyeres distributed symmetrically to the lower part of blast furnace, was chosen for analysis, with one tuyere chosen for modelling.

Combustion of coal was divided into five stages as described in the introduction: heating, drying, devolatilization, volatile combustion and residual char combustion. Devolatilization was modelled with the Kobayashi model [8], which is an empirical model based on two competing overall reactions. It is a widely used model in coal combustion. The volatile combustion model was based on GRI-MECH 1.2 [9,10], which contains 22 species and 104 reactions. The residual char combustion was described with reactions between char, oxygen, carbon dioxide and steam.

2.1. Geometry, mesh and boundary conditions

Geometry for the CFD model (Fig. 2) was created based on the BHP Billington-BlueScope Steel test rig [11]. The model was created with Ansys DesignModeler 16.0. It contained a blast pipe, a tuyere, a lance and a cylinder which models the raceway area. The inlet was placed in the beginning of the blast pipe and the outlet was in the end of the raceway. Inlets for the coal-nitrogen mixture (inner white circle) and cooling gas (outer white circle) were in the lance tip.

In the model, the diameters of the parts were as follows: the blast pipe was 110 mm, the tuyere tip was 70 mm, the lance was 1.27 mm with an outer the wall thickness of 1.6 mm, the cooling shroud diameter was 19.05 mm with the outer wall thickness of 1.6 mm, and the raceway was 300 mm. The tuyere tip was about 140 mm in the Raahe blast furnace; therefore, the difference to the real case was 50%. The lance was similar to the actual blast furnace.

For the CFD model the meshing was done with Ansys Meshing 16.0. The mesh consisted of about 713000 hexa- and tetrahedral computational cells. The mesh was dense in the tuyere area, where small surfaces exist as inlets for the cooling gas and nitrogen, and the velocity of the air blast is the highest.

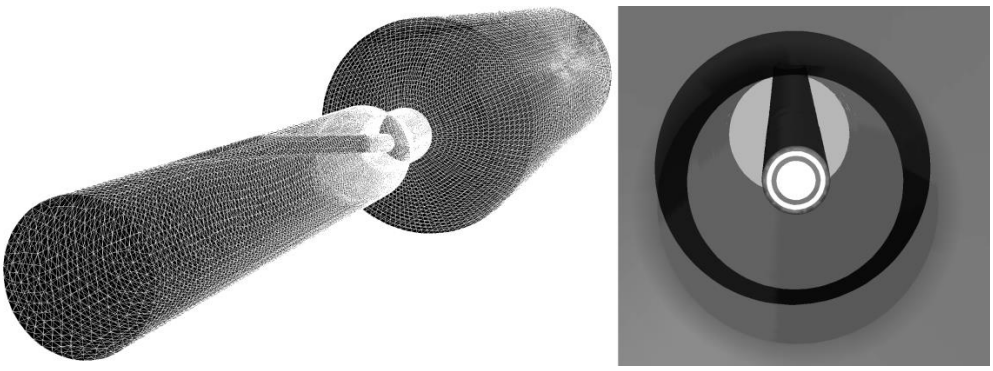

Figure 2. Geometry and the mesh of the CFD model.

The experimental rig was built to evaluate the potential of different injection coals and their use in the blast furnace [11]. Its operating conditions were not a perfect match for an actual blast furnace, but the velocity difference (about 40 m/s) between the air blast and the injected

PC was similar. Also, the temperature of the air blast was at the same level as it is in an actual blast furnace. Therefore, the heat and mass transfer phenomena should have been similar in both cases and it was reasonable to use the test rig to create the combustion model for the blast furnace. The pressure was the only variable in the experimental rig that was not set at a realistic level, because the pressurized system would have been too expensive (according to Mathieson et al. [11]). In the blast furnace in Raahe, the pressure is about 3.56 atm, and in the test rig 1 atm. Operating conditions for the simulation are presented in Table 1. These conditions are based on the paper written by Guo et al. [7]. Boundary conditions other than the coal type and the coal amount were kept the same in all the simulations.

Table 1. Operating conditions.

Air blast flowrate	300 Nm^3/h
Outlet pressure	1 atm
Temperature	1473 K
Coal temperature	323 K
Air blast O_2	21 vol-%
Cooling gas flowrate	3.2 Nm^3/h
Conveying gas flowrate	2.0 Nm^3/h
Cooling gas temperature	600 K
Conveying gas temperature	323 K

Proximate and ultimate analyses of the pulverized coals that were used in the simulation are given in Table 2. It can be seen that the coals were bituminous coals, but A was a medium volatile coal and coals B and C were high volatile coals [7,12].

Table 2. Proximate and ultimate analysis of coals.

	COAL A	COAL B	COAL C
Moisture w-%	1.20	3.20	3.60
Volatiles w-%	19.95	32.50	35.10
Ash w-%	9.70	9.80	6.20
Fixed carbon w-%	69.10	54.50	55.10
Sulphur w-%	0.34	0.58	0.41
C	89.10	83.50	82.60
H	4.70	5.30	5.44
O	4.10	8.60	9.50
N	1.70	1.95	2.15
S	0.37	0.60	0.30

The cumulative volume distribution of coal particles is presented in Fig. 3. The mean particle size in cases A, B, C were 30 µm, 40 µm and 40 µm, respectively. Particle sizes from 1 to 200 µm were used in the CFD model and they were divided into 12 groups. These distributions were approximated from Fig. 1, from Guo et al. [7], using the Weibull cumulative distribution function. The shape and scale parameters for coals A, B and C were 1, 43 µm, 1.1, 60 µm and 1.2, 56 µm, respectively. Injections were released from the coal lance surface at the same angle as the coal lance outlet.

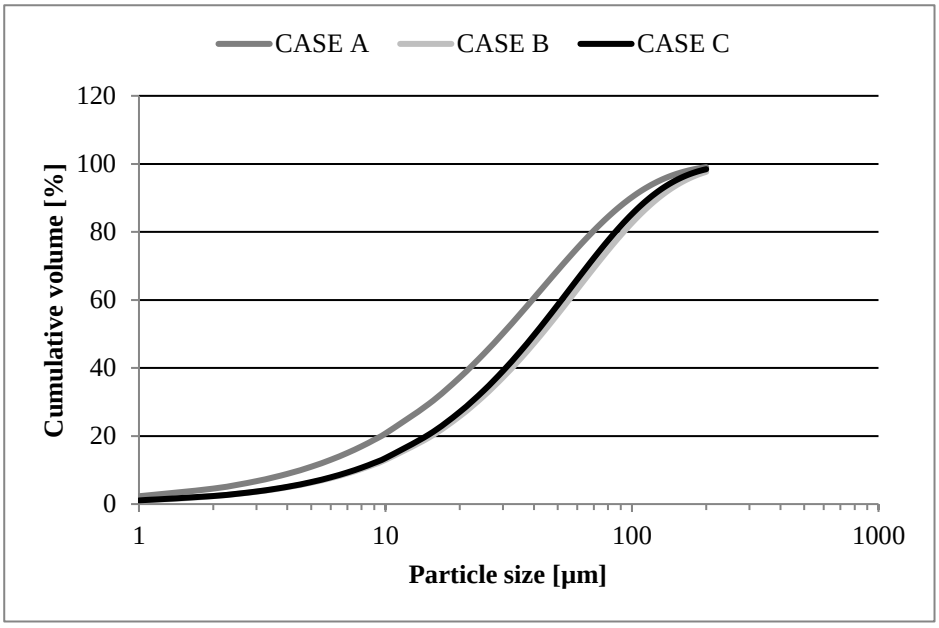

Figure 3. Cumulative volume distribution of coal particles.

2.2. Continuous phase

The CFD modelling was done with Ansys Fluent 16.0 [13]. It used the Finite Volume Method (FVM) to discretize the flow domain and the governing conservation equations were integrated over each computational cell. The continuity equation used is written as:

$$\frac{\partial \rho}{\partial t} + \nabla \cdot (\rho \vec{v}) = 0 \quad (1)$$

The momentum conservation equation in an inertial frame of reference was:

$$\frac{\partial}{\partial t}(\rho \vec{v}) + \nabla \cdot (\rho \vec{v} \vec{v}) = -\nabla p + \nabla \cdot \left(\mu \left[(\nabla \vec{v} + \nabla \vec{v}^T) - \frac{2}{3} \nabla \cdot \vec{v} I \right] \right) + \rho \vec{g} + \vec{F} \quad (2)$$

Turbulence was simulated with the realizable κ-ε model [14]. It is a two equation model, which is based on the modelled equations for the turbulence kinetic energy (κ) and its dissipation rate (ε). Realizability ensures the positivity of turbulent normal stresses and Schwartz' inequality between any of the fluctuating quantities [13,14]. It prevents the turbulence model from producing unphysical results. In the realizable κ-ε model, turbulent viscosity is calculated differently from the standard model, where C_μ is a constant. More information about the model can be found in the article written by Shih et al. [14].

2.3. Discrete phase

The discrete coal phase was modelled with the Lagrangian method. This method is used to study the behavior of an individual particle. In the Lagrangian method particle trajectories are computed for each particle separately and therefore the particle properties are known at each step. The particle force balance is written as:

$$\frac{dv_p}{dt} = F_D(\vec{v} - \vec{v}_p) + \frac{\vec{g}(\rho_p - \rho)}{\rho_p} + \vec{F} \quad (3)$$

where the drag force F_D is calculated for a spherical particle. Turbulent dispersion of the particles is taken into account with random the walk method [15].

The Lagrangian method makes it possible to calculate the burnout degree of all particles separately in their own size groups. The burnout degree B is calculated using Eq. 4:

$$B = \frac{1 - \frac{m_{a,0}}{m_a}}{1 - m_{a,0}} * 100\% \quad (4)$$

where $m_{a,0}$ is the ash content of the initial coal particle and m_a is the ash content at the current time step.

2.3.1. Particle drying

Coal particle moisture fractions varied between 1.2 to 3.6%. This was taken into account in calculations via droplet evaporation or via a boiling model, depending on the particle temperature. Evaporation was modeled with a convection and diffusion controlled model [16], which is meant for high Re flows, where convection is important.

$$\frac{dm_p}{dt} = k_c A_p \rho_\infty \ln(1 + \frac{Y_{i,s} - Y_{i,\infty}}{1 - Y_{i,s}}) \quad (5)$$

When the particle temperature reaches that of boiling water, Eq. 6 (for boiling) was used.

$$\frac{d(d_p)}{dt} = \frac{2}{\rho_p h_{fg}} [\frac{2k_{\infty[1+0.23\sqrt{Re_d}]}}{d_p}(T_\infty - T_p) + \varepsilon_p \sigma(\theta_R^4 - T_p^4)] \quad (6)$$

The particle temperature was calculated using a heat balance between the sensible heat change in the particle and the convective and latent heat transfer in the particle and the continuous phase.

2.3.2. Devolatilization

During particle heating, the volatile matter is released from the coal particle. The model for devolatilization was based on the two competing reactions, where reaction rate constants were defined for low and high temperature reactions. The reactions consume coal and produce char and volatiles. The model parameters were taken from the article written by Du & Chen [17]. These parameters had a good fit to their experimental data. Devolatilizing species were calculated from the coal proximate and ultimate analysis (Tables 2-3). To simplify the reaction model, sulphur and nitrogen were not taken into consideration in the calculations, whereas they were modified to be presented as $C_xH_yO_z$.

Low temperature devolatilization was treated as presented in Eq. 7:

$$Coal \xrightarrow{k_1} Char\ (1 - \alpha_1) + Volatile\alpha_1 \quad (7)$$

where α_1 is the volatile yield. High temperature devolatilization was calculated similarly, but α_2 was $1.5*\alpha_1$:

$$Coal \xrightarrow{k_2} Char(1 - \alpha_2) + Volatile\alpha_2 \quad (8)$$

The rate constants k_1 and k_2 for the devolatilization were calculated from the Arrhenius equation, where A_1, E_1, A_2 and E_2 are 3.7E5, 7.4E7 J/kmol, 1.46E13 and 2.51E8 J/kmol, respectively. [17]

The volatiles cracking method for smaller components is presented in Eq. 9:

$$C_xH_yO_z \rightarrow \frac{x - z}{2} C_2H_4 + \frac{y - 4x}{2} H_2 + zCO \quad (9)$$

The Arrhenius parameters [18] for the cracking were A = 2.119E11 and E = 2.027E8 J/kmol, taken from the Fluent coal calculator kinetics for two step coal combustion.

2.3.3. Char oxidation

Char consumption is a very significant part of the coal reaction process. When considering coal combustion, it is the most time-consuming part. It is known that low-rank coal chars are more reactive than high-rank coal chars and thus a single model cannot explain all of the coal types accurately [18]. In this model the approximation was, however, based on the data collected from coals similar to the experimental coal. Char reactions occur between solid carbon and gas phase species. In this case the species were O_2, CO_2 and H_2O. During combustion the particle diameter remains constant, but the density lowers as the combustion degree progresses.

The exothermic partial oxidation of char with O_2 is presented in Eq. 10. Gasification Equations 11 – 12 are endothermic, requiring heat, and they occur more easily when the temperature increases.

$$2C + O_2 \xrightarrow{k_3} 2CO \quad (10)$$

$$C + CO_2 \xrightarrow{k_4} 2CO \quad (11)$$

$$C + H_2O \xrightarrow{k_5} CO + H_2 \quad (12)$$

The Arrhenius parameters A_3, E_3, A_4, E_4, A_5 and E_5 [19] for the Equations 10 – 12 were 2.013, 7.9818E7 J/kmol, 3.1, 1.31E8 J/kmol, 1.33 and 1.15E8 J/kmol, respectively.

2.4. Gas phase reactions

In the blast furnace raceway the highest temperature is around 3000 K and the stoichiometric ratio is between 0.5 and 0.8 [2], which means that gasification reactions are important, because the mixture is fuel-rich and reactions occur through radicals. To model gasification and radical reactions a finite rate combustion model is needed; the Eddy Dissipation Concept (EDC) was chosen. The volatile combustion model was GRI-MECH 1.2 [9,10], which contains 22 species and 104 reactions. The reaction mechanism is available online [10]. The CHEMKIN-CFD solver was used to calculate chemical reactions.

In EDC it is assumed that most of the reactions take place in the smallest scales of the turbulence, which are called the fine structures. These fine structures are treated as well-stirred reactors. In Fluent, each computational cell is treated as a constant pressure reactor, where the initial conditions are the current species and temperature inside the cell.

2.5. Heat transfer

Forced convection dominated heat transfer in the test rig, because the air blast velocity could be over 120 m/s in the front of the tuyere. There were large differences (maximum 2477 K) in temperatures in the test rig, and the forced convection was weaker after the PC velocity increased. Because of this, the radiation heat transfer was included in the computation, and the Discrete Ordinates method (DO) was chosen to model it. The model includes as well the effect of the gray gases. PC and walls were assumed to be black bodies. The particle

scattering factor was set to 0.9, which is the recommended value for the coal combustion modelling in the user's guide [18]. Adding the PC radiation interaction meant ignoring the scattering in the continuous phase.

3. Results and discussion

The observation plane for sampling was the cross section 1 m downstream from the tip of the injection lance. The measurements of the burnout degree in the test rig were done at the same spot. Results from the CFD calculations were compared to the experimental results from the literature [7] in Table 3. It can be seen that the burnout degree matches well with the experimental results. Results varied a little with different coal types. When the modelling was done with the A1 setup, the burnout degree was 64.8%, which overestimates the combustion degree by 1.7%. With the B1 setup, the CFD produced a result that underestimates the burnout degree by about 5.3%. In the C1 setup, the model results differed only 4.1% from the experimental results. The B3 setup produced the most accurate results, the experimental results and CFD not differing from each other in the first decimal. In this case the injection level was the highest, which is most important when considering the actual blast furnace case. The worst results were from the case A2, where the difference was 7.3%. According to Ishii [2], the burnout degree should be at least 70% to ensure a stable blast furnace process when the injection rate is about 200 kg/ton of hot metal (thm), and this may have been a cause of the difference.

Table 3. Calculated and experimental burnout of coal particles.

Case	Flowrate [kg/h]	VM [%]	Stoichiometric ratio	Burnout experimental [%]	Burnout CFD [%]
Coal A1	25.2	20.19	1.20	63.7	64.8
Coal A2	35.9	20.19	0.84	55.5	59.9
Coal B1	25.5	33.57	1.25	81.5	77.2
Coal B2	40.0	33.57	0.80	75.5	74.8
Coal B3	46.7	33.57	0.68	71.4	71.4
Coal C1	23.5	36.41	1.37	78.9	75.7
Coal C2	35.1	36.41	0.92	76.2	71.5

From Table 3 it can be seen that the stoichiometric ratio had a strong effect on the PC burnout. The results show that cases with fuel-lean combustion conditions led to a higher burnout of the PC than fuel-rich conditions. The probability of collision and reaction between oxygen and fuel molecules increases with an increasing stoichiometric ratio. Oxygen that does not react with PC in the blast furnace will react with coke, which increases the fuel costs. The minimum stoichiometric ratio in the blast furnace is 0.70 to 0.75, below which blast furnace operation becomes unstable [2].

The combustion degree was strongly dependent on the particle size (Fig. 4). Almost all of the particles below 40 µm had enough time to burn during the 1 m flight. The biggest particles (200 µm) in the cases Coal A1, B3 and C1 had much lower burnout degrees of about 31.3%, 42.7% and 45.2%, respectively. The burnout degree increased as the level of volatile matter got higher, since the devolatilization was faster than char combustion.

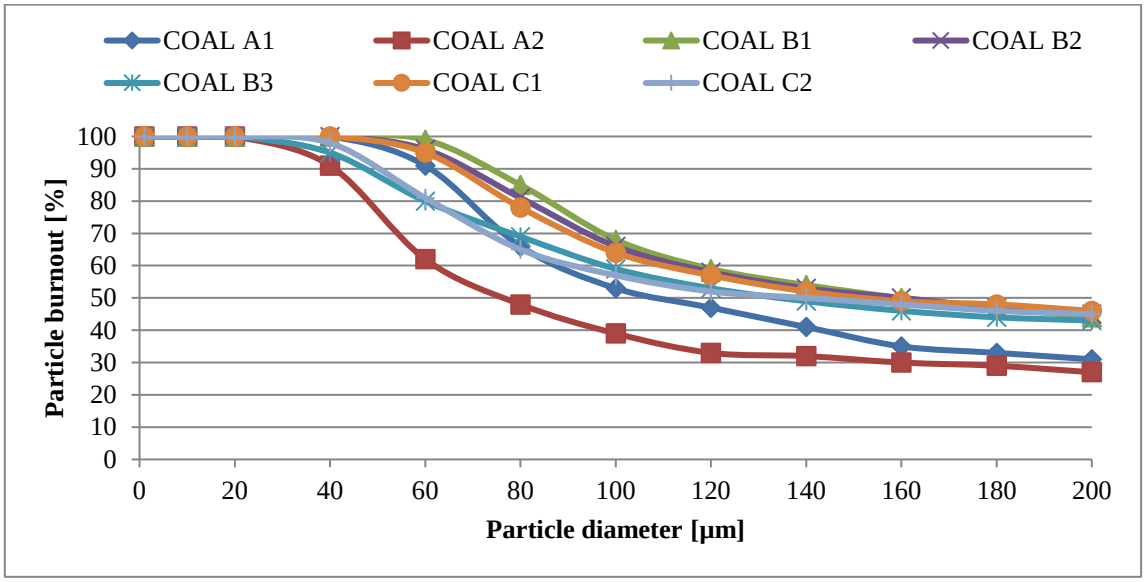

Figure 4. Effect of particle size on combustion degree.

These results show that the model overestimated particle combustion with oxygen when the medium volatile matter coal was used and underestimated the reaction rate in lower rank coals. Since the model is time-dependent, the results can be related to that also. Mixing changes a little during calculation, which might lead to different results from the experimental measurements. Changes in mixing are minimized with long sampling times and large sampling sizes over 20 000 particles.

The moisture fraction in the PC was small, which means particles dried quickly (maximum 3 ms). Devolatilization of PC (Coal B) is presented in Fig. 5. Particle sizes are based on the groups set as boundary values. Small particles lost their volatile matter quickly, but for the larger particles complete devolatilization took about 0.035 seconds. Devolatilization time increased linearly with the particle diameter.

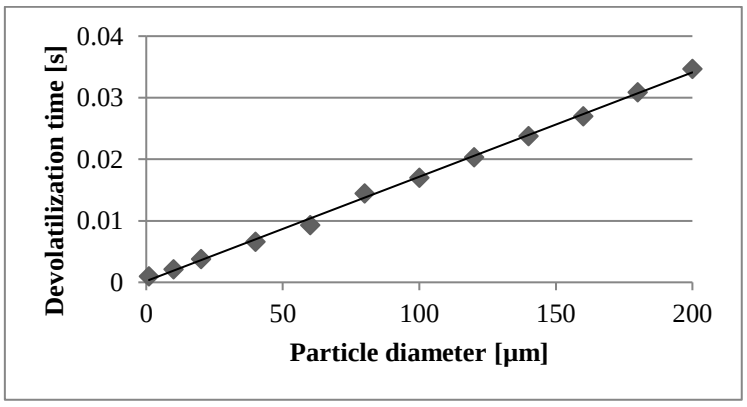

Figure 5. Particle devolatilization time.

The particle residence time in the system affected the combustion degree and was dependent on the particle size, because larger particles accelerate slower. The typical time that an average particle spent in the test rig was between 0.03 to 0.06 seconds, which is very short time when considering PC combustion. Because of this, the particle burnout with medium volatile coal A was only about 60%. Because the residence time is short, the mixing between PC and air blast should be optimized to increase the burnout degree of the PC particles.

The velocity at the tuyere nose both 3 cm above and below the centre was about 128 m/s (Fig. 6), which matches well with the results from the same geometry by Shen et al. [20]. The PC lance (Z-axis 0.53 m) created an obstacle to the centre of the tuyere, which decreased the cross-sectional area of the tuyere and led to an increased velocity at the tuyere exit. At the centre the velocity was also lower, because of the retarding effect of the PC on the air blast. This was a result of the poor mixing, which is a well-known problem in PC injection systems.

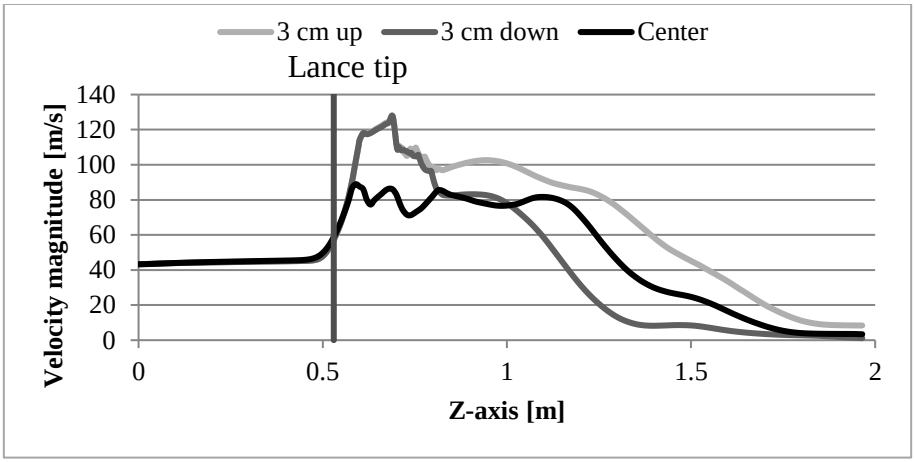

Figure 6. Air blast velocity along z-axis.

Small particles released their volatile matter quickly, with combustion starting only 4 cm from the lance tip (Z-axis 0.53 m) (Fig. 7), consuming all the available oxygen from the PC dust cloud. Gaseous combustion reached a maximum temperature of about 2800 K, which seems reasonable when compared to the blast furnace study [21] which used a probability density function combustion model. Combustion occurs on the surface of the PC dust cloud and mostly devolatilization takes place in the centre of the flow. Mixing diluted the PC cloud enough to ignite the mixture in the centre line about 60 cm from the lance tip so that the temperature reached 2500 K, but the hottest temperatures were located 80 cm from the lance tip.

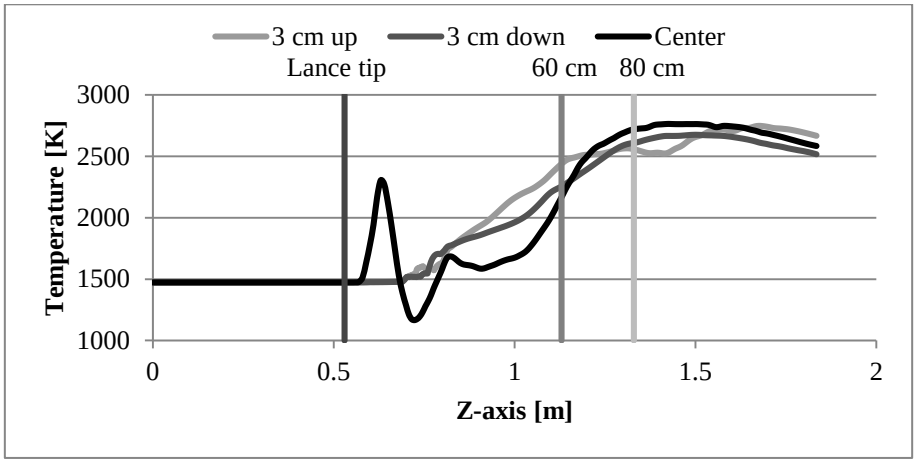

Figure 7. Gas temperature along z-axis.

The experimental rig was not a perfect match for the actual blast furnace and was meant chiefly to evaluate combustion of different types of coals and their suitability as an injection material. The pressure difference between Raahe's blast furnace and the test rig was about 2.56 atm. Increased pressure leads to higher reaction rates and creates uncertainty in the combustion model. Another cause for possible errors is that there was no public gas phase measurement data available and thus the model could not be validated. The velocity difference between the air blast and PC after injection was on the same level in the test rig and the blast furnace. Therefore, the heat and mass transfer phenomena between continuous and discrete phases were similar. This is very important, because ignition should not take place in the tuyere area in the blast furnace, as it creates wear and ablation of the tuyere walls. The model predicted that the PC particles with a diameter less than 10 µm release their volatiles quickly after the injection and ignite close to the lance tip. This behaviour should be modelled and validated in an actual blast furnace.

4. Conclusions

The work in this paper focused on model creation and CFD modelling of combustion of PC in the blast furnace tuyere-raceway area of a test rig. The particle combustion degree was studied with three different types of coals and compared with the results from the existing literature. The amount of injected PC was also varied.

The combustion model consisted of five steps, i.e. heating, drying, devolatilization, char combustion and gas phase combustion. CFD modelling predicted the combustion degree to a reasonable accuracy when compared to the experimental results. In the A2 case, the difference between experimental and computational results was 7.3%, which was the worst result. The best case was B3, where the difference was less than 1%. On average, the difference was about 3.6%. Lower rank coals have more reactive char than high rank coals, which can be seen from the results. The model overestimated the coal A reaction rate and underestimated the reaction rate of the coals B and C.

The residence time was less than 0.06 seconds in the tuyere-raceway area, which produced challenges for good combustion. This is why the mixing between fuel and air blast should be optimized when the aim is to increase combustion efficiency.

The maximum temperature was about 2800 K, which was in good agreement with the literature. Based on the results, this model can be used to study limiting factors of combustion and gasification of PC in a blast furnace. This combustion model can be added to a more comprehensive CFD model of the blast furnace tuyere-raceway area.

Acknowledgements

This work was performed as a part of Finnish Metals and Engineering Competence Cluster (FIMECC)'s System Integrated Metals Processing (SIMP) program. The authors wish to acknowledge CSC – IT Center for Science, Finland, for computational resources.

Notation

A_i	pre exponential factor for the reaction i	Re_d	particle Reynolds number [-]
A_p	particle surface area [m^2]	T_p	particle temperature [K]
B	burnout degree [%]	t	time [s]
d_p	particle diameter [m]	T	temperature [ºC]
E_i	activation energy for the reaction i [J/kmol]	T_∞	continuous phase temperature [K]
$\vec{F}$	External body forces [N]	$\vec{v}$	velocity vector [m/s]
F_D	drag force [N]	$\vec{v}_p$	Particle velocity [m/s]
g	gravity [m/s^2]	$Y_{i,s}$	vapour mass fraction at the surface [-]
h_{fg}	latent heat [J/kg]	$Y_{i,\infty}$	vapour mass fraction in the bulk gas [-]
k_c	mass transfer coefficient [m/s]	α_i	yield factor [-]
k_i	reaction rate constant of reaction i	ε_p	particle emissivity [ ]
m_a	ash content of the current time step [%]	θ_R	radiation temperature [K]
$m_{a,0}$	ash content of the initial coal particle [%]	ρ	density [kg/m^3]
m_p	particle mass [kg]	ρ_p	droplet density [kg/m^3]
p	pressure [Pa]	ρ_∞	bulk gas density [kg/m^3]
R	universal gas constant [J/kmolK]	σ	Stefan-Boltzmann constant [$W/m^2/K^4$]
Re	Reynolds number [-]	PC	pulverized coal

References

[1] Vuokila, A., Riihimäki, M. & Muurinen, E. 2014. CFD-modeling of heavy oil injection into blast furnace – Atomization and mixing in Raceway-Tuyere area. Steel Research International, 11, 1544-1551.

[2] Ishii, K. 2000. Advanced pulverized coal injection technology and blast furnace operation. Elsevier/Pergamon, Oxford.

[3] Nightingale, R., Dippenaar, R. & Lu, W. 2000. Developments in blast furnace process control at port kembla based on process fundamentals. Metallurgical and Materials Transactions, 31, 993-1003.

[4] Shen, Y., Shiozawa, T., Austin, P. & Yu, A. 2014. Model study of the effect of bird's nest on transport phenomena in the raceway of an ironmaking blast furnace. Minerals Engineering, 0, 91-99.

[5] Santos, B. O. d. A., Maia, B. T., Garajau, F. S., Guerra, M. d. S. L., Assis, P. S. & Barros, J. E. M. 2014. A new concept of auxiliary fuel injection through tuyeres in blast furnaces developed by numerical simulations. Journal of Materials Research and Technology, 2, 142-149.

[6] Gu, M., Chen, G., Zhang, M., Huang, D., Chaubal, P. & Zhou, C. Q. 2010. Three-dimensional simulation of the pulverized coal combustion inside blast furnace tuyere. Applied Mathematical Modelling, 11, 3536-3546.

[7] Guo, B., Zulli, P., Rogers H., Mathieson, J. G. & Yu, A. 2005. Three-dimensional simulation of flow and combustion for pulverised coal injection. ISIJ International, 9, 1272-1281.

[8] Kobayashi, H., Howard, J. B. & Sarofim, A. F. 1977. Coal devolatilization at high temperatures. Symposium (International) on Combustustion, 1, 411-425.

[9] Frenklach, M., Wang H., Goldenberg, M., Smith, G. P., Golden D. M., Bowman, C. T., Hanson. R. K., Gardiner, W. C. & Lissianski, V. 1995. GRI-Mech – An optimized detailed chemical reaction mechanism for methane combustion. Gas Research Institute, Report No. GRI-95/0058.

[10] Frenklach, M., Wang H., Yu, C. -L, Goldenberg, M., Bowman, C. T., Hanson. R. K., Davidson D. F., Chang, E. J., Smith, G. P., Golden D. M., Gardiner, W. C. & Lissianski, V. 1995. http://www.me.berkeley.edu/gri_mech/.

[11] Mathieson, J. G., Truelove, J. S. & Rogers, H. 2005. Toward an understanding of coal combustion in blast furnace tuyere injection. Fuel, 10, 1229-1237.

[12] Carpenter, A. M. & IEA Coal Research. 1988. Coal Classification. IEA Coal Research.

[13] Ansys Inc. 2014. Ansys Fluent 16.0 Theory Guide. Ansys Inc, USA.

[14] Shih, T., Liou, W., Shabbir, A., Yang, Z. & Zhu, J. 1994. A new k-epsilon eddy viscosity model for high Reynolds number turbulent flows: Model development and validation. Computers and Fluids, 3, 227-238.

[15] Gosman, A. D. & loannides, E. 1983. Aspects of Computer Simulation of Liquid-Fueled Combustors. Journal of Energy, 6, 482-490.

[16] Sazhin, S. S. 2006. Advanced Models of Fuel Droplet Heating and Evaporation. Progress in Energy and Combustion Science, 32, 162-214.

[17] Du, S. & Chen, W. 2006. Numerical prediction and practical improvement of pulverized coal combustion in blast furnace. International Communications in Heat and Mass Transfer, 3, 327-334.

[18] Ansys Inc. 2014. Ansys Fluent 16.0 User's Guide. Ansys Inc, USA.

[19] Bartok, W. & Sarofim, A. F. 1991. Fossil fuel combustion: a source book, John Wiley, New York.

[20] Shen, Y. S., Guo, B. Y., Yu, A. B. & Zulli, P. 2009. A three-dimensional numerical study of the combustion of coal blends in blast furnace. Fuel, 2, 255-263.

[21] Du, S., Yeh, C., Chen, W., Tsai, C. & Lucas, J. A. 2015. Burning characteristics of pulverized coal within blast furnace raceway at various injection operations and ways of oxygen enrichment. Fuel, 0, 98-106.

